

## Preparation of Silicon-Based Intermetallic Nanoparticles in Induction Thermal Plasmas

(Dept. Env. Chem and Tech, Tokyo Inst. Tech.) OT.Watanabe, M.Shigeta

Numerical analysis is conducted for disilicide nanoparticle preparation in induction thermal plasmas. In Mo-Si system, nuclei of Mo are produced and grow in the upstream region and then Si vapor condenses on the Mo particles. The composition shows wide range when condensations of metal and silicon occur at the different positions. On the other hand, it shows narrow range when condensations of metal and silicon occur simultaneously. The difference of the formation mechanisms leads to the preparation of MoSi<sub>2</sub> as well as the sub-products such as Mo<sub>5</sub>Si<sub>3</sub> and Si.

E-mail: [watanabe@nr.titech.ac.jp](mailto:watanabe@nr.titech.ac.jp)

### 1. INTRODUCTION

The preparation of nanoparticles with high purity can be easily achieved by induction thermal plasmas (ITPs) since they have high enthalpy, large plasma volume, high chemical reactivity and high quenching rate [1]. In the tail of the ITP where the quenching rate is high (10<sup>5</sup>-10<sup>6</sup> K/s), homogeneous nucleation occurs at different positions due to the differences of the saturation vapor pressures and the surface tensions of the materials [2]. After homogeneous nucleation, the mixed vapors of metal and silicon condense on the nuclei. In the present study, numerical analysis is conducted for the preparation of silicon-based intermetallic nanoparticles in the ITPs.

### 2. NUMERICAL MODEL

#### 2.1 ITP model

The ITP model is proposed on the following assumptions [1]. The thermofluid field is steady, laminar and 2D axisymmetric. The induction electromagnetic fields in the ITP are considered 2D axisymmetric with negligible displacement currents. Gravitational forces and viscous dissipation are negligible. The state of the ITP is optically thin and electrically neutral.

The governing equations of continuity, momentum, energy, and plasma species per unit volume are summarized in the following general form in cylindrical coordinates:

$$\frac{\partial}{\partial z}(\rho u \phi) + \frac{1}{r} \frac{\partial}{\partial r}(r \rho v \phi) = \frac{\partial}{\partial z} \left( \Gamma \frac{\partial \phi}{\partial z} \right) + \frac{1}{r} \frac{\partial}{\partial r} \left( r \Gamma \frac{\partial \phi}{\partial r} \right) + S \quad (1)$$

where  $\phi$  corresponds to physical variables such as  $u$ ,  $v$ ,  $w$ ,  $h$ , and  $n$ .

The governing equation of the induction electromagnetic fields is expressed as [3]

$$\frac{\partial^2 A_\theta}{\partial z^2} + \frac{1}{r} \frac{\partial}{\partial r} \left( r \frac{\partial A_\theta}{\partial r} \right) - \frac{A_\theta}{r^2} = i \mu_0 \sigma_e \omega A_\theta \quad (2)$$

where  $i$  is equal to  $\sqrt{-1}$ . The induction electromagnetic fields are represented using the electromagnetic vector potential to consider the interaction between the applied electromagnetic field of the coils and the induction electromagnetic field of the plasma.

#### 2.2 Nanoparticle preparation model

The vapor pressures of the metal and silicon reach higher than the saturation pressure (supersaturation) due to the rapid temperature decrease of the plasma gas, which causes the particle creation by homogeneous nucleation and heterogeneous condensation growth. In the present study, a one-dimensional multi-component model is proposed to clarify the formation

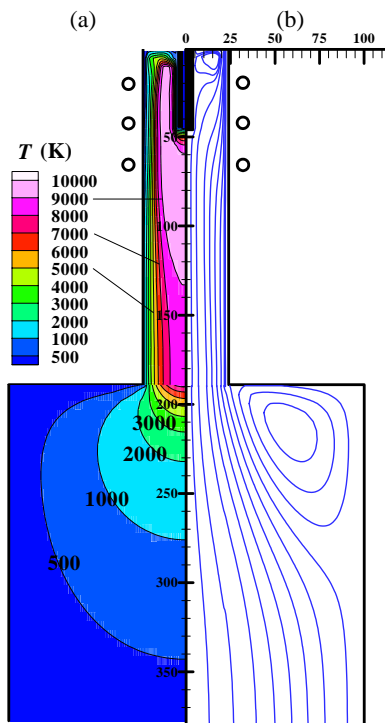


Fig.1 Thermofluid fields:  
(a) Temperature, (b) Streamlines

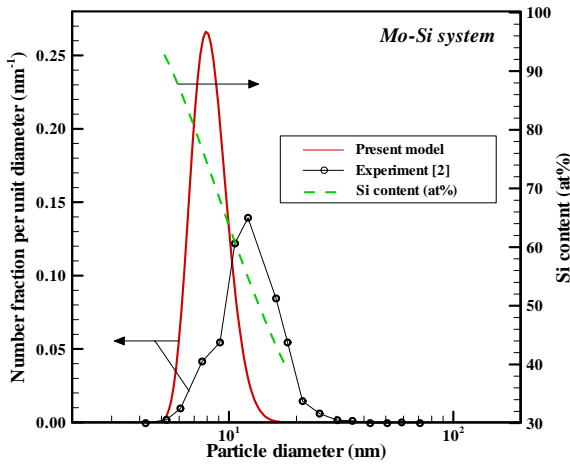


Fig.2 Particle size distribution and Si content for Mo-Si systems

mechanism of silicon-based intermetallic nanoparticles with the following assumptions. The produced nanoparticles are spherical. The particle inertia can be neglected due to the small size and the velocity of the condensing phase and the condensed phase is the same as that of the plasma gas. The temperature of the nanoparticles is the same as that of the plasma gas and the heat generation caused by condensation is neglected. The vapors of the metal and silicon are considered as ideal gases. The agglomeration among the nanoparticles is negligible. The total pressure in the reaction chamber is atmospheric.

Supersaturated vapor creates nuclei by homogeneous nucleation. Homogeneous nucleation rate is proposed by [4]

$$J_i = \frac{(\beta_{11})_i n_{si}^2 S_i}{12} \sqrt{\frac{\Theta_i}{2\pi}} \exp\left(\Theta_i - \frac{4\Theta_i^3}{27(\ln S_i)^2}\right) \quad (3)$$

where  $S$ ,  $\Theta$  and  $\beta_{11}$  are the supersaturation ratio, the normalized surface tension and the collision frequency function between the monomers, respectively.

In the state of the high concentration of the particles and the low supersaturation, heterogeneous condensation occurs on the surface of the nuclei, which results in the nanoparticle growth. The rate of the particle growth by heterogeneous condensation is estimated from the net molecular flux from the vapors to the condensed phase considering all the range of Knudsen number [5]

$$\frac{d(d_{pi})}{dt} = \sum_j \frac{4\rho_g}{d_{pi}\rho_{cj}} D_j (X_{1j} - X_{sj}) \left\{ \frac{1 + Kn_i}{1 + 1.7Kn_i + 1.333Kn_i^2} \right\}. \quad (4)$$

The subscript  $i$  and  $j$  represent the species of the vapors.

### 3. RESULTS AND DISCUSSION

Figure 1 shows the thermofluid fields in the ITP torch and the reaction chamber. Due to the Joule heating generated by the applied electromagnetic power, the remarkably high temperature zone (10,000 K) exists in the ITP torch. In the reaction chamber, the temperature decreases drastically ( $10^5 - 10^6$  K/s), which results in a great promotion of particle nucleation. The ITP torch also has recirculation region due to the radial Lorentz force.

Figure 2 shows the finally obtained particle size distribution with the number mean diameter around 10 nm and silicon content for the particle diameters in Mo-Si systems. The particle size distribution obtained from the present model shows a good agreement with the experiment [2]. Molybdenum nucleates and grows earlier and then silicon condenses on molybdenum particles. Silicon content shows a wide range (40 - 94 %) which is determined by the balance between the original molybdenum content and the condensation amount of silicon vapor. The composition shows wide range when condensations of metal and silicon occur at the different positions. On the other hand, it shows narrow range when condensations of metal and silicon occur simultaneously. Compared with the phase diagram, molybdenum-disilicide  $\text{MoSi}_2$  as well as the sub-products such as  $\text{Mo}_5\text{Si}_3$  and Si are prepared.

### REFERENCES

- [1] M. Shigeta, T. Watanabe and H. Nishiyama: *Thin Solid Films*, **192**, 457 (2004)
- [2] T. Watanabe, H. Okumiya: *Science and Technology of Advanced Materials*, **5**,639 (2004).
- [3] J. Mostaghimi and M. I. Boulos: *Plasma Chem. Plasma Proc.*, **9**, 25 (1989)
- [4] S. L. Girshick, C. P. Chiu and P. H. McMurry: *Aerosol Science and Technology*, **13**, 465 (1990)
- [5] S. V. Joshi, Q. Liang, J. Y. Park, J. A. Batdorf: *Plasma Chem. Plasma Proc.*, **10**, 339 (1990)